JPL-ANTOPT Antenna Structure Optimization Program

D. M. Strain

Ground Antennas and Facilities Engineering Section

New antenna path-length error and pointing-error structure optimization codes were recently added to the MSC/NASTRAN structural analysis computer program. Path-length and pointing errors are important measures of structure-related antenna performance. The path-length and pointing errors are treated as scalar displacements for statics loading cases. These scalar displacements can be subject to constraint during the optimization process. Path-length and pointing-error calculations supplement the other optimization and sensitivity capabilities of NASTRAN. The analysis and design functions were implemented as "DMAP ALTERs" to the Design Optimization (SOL 200) Solution Sequence of MSC-NASTRAN, Version 67.5.

I. Introduction

For many years, the principal antenna structural design tool of the Ground Antennas and Facilities Section has been the JPL-IDEAS Design Optimization Program [1]. It has proved very useful both as a design tool and as a test-bed for numerous analytical and optimization techniques. It has also taken advantage of numerous unique features of the FORTRAN-V compilers of the UNISYS machines. While this was expedient, it has proved increasingly restrictive. Costs have increased, maintainability has suffered, and the code is not "portable."

JPL-IDEAS depends on a limited repertoire of finite elements, both for computational efficiency and to effect the optimization algorithms. The NASTRAN structural analysis computer program has traditionally been used to check IDEAS results and for analyses that required a more extensive element library. Having to maintain parallel finite-element models was at best cumbersome and time consuming. With the advent of design optimization capabilities in MSC/NASTRAN, and the rumored imminent departure of the UNISYS platforms, it was decided to implement the essential features of IDEAS directly into MSC/NASTRAN.

II. Analysis Capabilities

A. Surface Accuracy Calculations

Antenna primary surface accuracy can be represented as the weighted root-mean-square (rms) error of a paraboloid best fitting the deformed reflector surface in a half-path-length sense [2,3]. A subset of the finite-element model grid points is chosen to represent the primary-reflector panel support points. Each of these grid points is assigned a weighting function proportional to the reflector panel area it supports.

The following is a summary of the path-length error calculations for one loading case. Matrix and vector quantities are noted with their dimensions in square brackets, where N is the size of the weighted grid subset. Quantities designated as "raw" refer to errors with respect to the undeflected, nominal paraboloid; those designated as "fit" are errors with respect to the best-fitting paraboloid. The other symbols are defined as

$$
\begin{aligned}
f &= \text{nominal focal length of main reflector} \\
\mathbf{X, Y, Z} &= \text{spatial coordinates of the main reflector support points } [N \times 1] \\
\mathbf{U, V, W} &= \text{translation displacement components } [N \times 1] \\
\mathbf{wgt} &= \text{diagonal matrix of surface panel weighting function } [N \times N] \\
\sum wgt &= \text{sum of the surface panel weights} \\
\rho &= \text{raw path-length errors, with respect to nominal paraboloid } [N \times 1] \\
\mathbf{gX, gY, gZ} &= \text{direction cosines of surface normal vectors } [N \times 1] \\
\mathbf{A} &= \text{basis functions of normal equations, } \mathbf{wgtAS} = \mathbf{wgt}\rho \; [N \times 6] \\
\mathbf{S} &= \text{solution of normal equations } [6 \times 1] \\
\phi &= \text{fit path-length errors, with respect to best-fit paraboloid } [N \times 1]
\end{aligned}
$$

$$
\rho_i = \frac{-2f\mathbf{X}_i\mathbf{U}_i - 2f\mathbf{Y}_i\mathbf{V}_i + 4f^2\mathbf{W}_i}{\mathbf{X}_i^2 + \mathbf{Y}_i^2 + 4f^2}
$$

$$
rms_{raw} = \left(\frac{\rho_i^T \mathbf{wgt}_i \rho_i}{\sum wgt} \right)^{1/2}
$$

$$
\mathbf{gX}_i = \frac{-\mathbf{X}_i}{\mathbf{X}_i^2 + \mathbf{Y}_i^2 + 4f^2}
$$

$$
\mathbf{gY}_i = \frac{-\mathbf{Y}_i}{\mathbf{X}_i^2 + \mathbf{Y}_i^2 + 4f^2}
$$

$$
\mathbf{gZ}_i = \frac{2f}{\mathbf{X}_i^2 + \mathbf{Y}_i^2 + 4f^2}
$$

$$
\mathbf{A}_i = [-\mathbf{gZ}_i\mathbf{gX}_i \quad -\mathbf{gZ}_i\mathbf{gY}_i \quad -\mathbf{gZ}_i\mathbf{gZ}_i \quad -\mathbf{Z}_i\mathbf{gZ}_i\mathbf{gZ}_i \quad (\mathbf{Z}_i\mathbf{gZ}_i\mathbf{gY}_i - \mathbf{Y}_i\mathbf{gZ}_i\mathbf{gZ}_i)
$$

$$
(-\mathbf{Z}_i\mathbf{gZ}_i\mathbf{gX}_i + \mathbf{X}_i\mathbf{gZ}_i\mathbf{gZ}_i)]
$$

$$
\mathbf{S} = [\mathbf{A}^T\mathbf{wgtA}]^{-1}\mathbf{wgt}\rho
$$

$$
\phi = \rho - \mathbf{AS}
$$

$$
rms_{fit} = \left(\frac{\phi^T \mathbf{wgt}\phi}{\sum wgt} \right)^{1/2}
$$

The six rows of the solution vector $\mathbf{S}$ are the X, Y, and Z translational offsets of the vertex of the best-fitting paraboloid; the change in focal length of the best-fitting paraboloid; and the rotational offsets of the best-fitting paraboloid about the x- and y-axes.

The coefficient matrix ($[\mathbf{A}^T \mathbf{wgt A}]$), the right-hand side ($\mathbf{wgt}\rho$), and solution ($\mathbf{S}$) are printed and other results of the path-length analysis are tabulated for each loading case.

B. Pointing Error Calculations

The pointing error is calculated as the sum of the error contributions from each of the optical components of the antenna: the primary reflector, the secondary reflector (S/R), and the microwave-feed phase center [4]. The errors due to the displacements of the primary reflector are calculated from the fitting parameters of the best-fit paraboloid (BFP). The motions of the secondary reflector are taken to be those of a grid point whose *motions* approximate the motions of the secondary. Similarly, the motions of the feed phase center are taken from the *motions* of a designated "feed" grid point. The spatial coordinates of these grids are not considered during pointing-error calculations. The symbols are defined as

$$
\begin{aligned}
K &= \text{beam deviation angle of primary reflector} \\
K_2 &= \text{beam deviation angle of secondary reflector} \\
M &= \text{magnification factor} \\
A, C &= \text{Cassegrain geometry parameters, where hyperboloid eccentricity} = C/A \\
F &= \text{focal length of nominal paraboloid} \\
dX, dY, dZ &= \text{translational offsets of BFP} \\
dF &= \text{change in focal length of main reflector paraboloid } (f_{BFP} - f_{nominal}) \\
rX, rY &= \text{rotational offsets of BFP or secondary reflector}
\end{aligned}
$$

Angular errors due to primary (BFP) motion in a symmetric Cassegrain system are calculated as follows:

Motion component	X-axis error	Y-axis error
Lateral translation	$-K/F \times dY$	$K/F \times dX$
Rotation	$(1 + K) \times rX$	$(1 + K) \times rY$

Errors due to secondary reflector motion in a symmetric Cassegrain system are calculated as follows:

Motion component	X-axis error	Y-axis error
Lateral translation	$(K/F - K2/F/M) \times dY$	$-(K/F - K2/F/M) \times dX$
Rotation	$-(2 \times (C - A) \times K/F) \times rX$	$-(2 \times (C - A) \times K/F) \times rY$

Errors due to feed phase center motion in a symmetric Cassegrain system are calculated as follows:

Motion component	X-axis error	Y-axis error
Lateral translation	$(K/M - 1/F) \times dY$	$-(K/M - 1/F) \times dX$

No pointing error accrues from axial motions or focal-length change of the components in a symmetric system.

The pointing error about the elevation axis can be predicted relative to the elevation-axis position transducer. The rotation of the grid point, whose rotation represents that of the transducer, is subtracted from the total pointing error about the x-axis and is reported as the "corrected" pointing error.

The default antenna-pointing analysis calculations assume a symmetric Cassegrain configuration: a paraboloidal main reflector and a hyperboloidal secondary reflector with coincident foci, and a point source microwave feed located at the other focus of the hyperboloid. Simple descriptions of this geometry are sufficient input for this traditional DSN case. For non-Cassegrain or asymmetric (e.g., clear-aperture) antenna configurations, the pointing-error calculations shown above can be overridden for each of the motions of each of the optical components. Components whose override factors have values of 0.0 (the default) will be calculated as outlined above. If the factor is other than 0.0, the pointing error will be the factor times the specified displacement.

Pointing errors about each axis are tabulated for each loading case with the results of the path-length analysis.

III. New Input Data

Although many NASTRAN input data (over those required for a simple statics run) are required to characterize the antenna for the new program, the amount of additional work required of the user has been kept to a minimum by automating the data preparation. Four simple data generation programs are available, each of which is written in standard FORTRAN.

The identification of the main reflector surface panel–support grids and of grids that represent the motions of the secondary reflector, feed phase center, and elevation transducer is accomplished through the use of NASTRAN DMIG, USET, and PARAM bulk data cards [5].

Two other programs can be used to generate the "DESVAR" and "DVPREL1" NASTRAN cards, required for sensitivity and optimization, from a list of element property cards. One of the programs recognizes PROD, PBAR, PBEAM, and PSHELL cards and generates cards whose design variable-to-property relation is cross-sectional area for the bar elements and thickness for the shells. The second program recognizes PBAR and PBEAM cards and generates design variables and relations suitable for rectangular tubes. The outside dimension and wall thickness are the design variables. These programs can be adapted easily to process other properties or output other design variables.

These additional data cards need only be generated once for a particular antenna configuration. The small amount of additional input (6 through 16 PARAMeters describing antenna geometry and pointing coefficients and four data cards per design constraint) can be generated easily by hand.

Surface accuracy and pointing error responses are each calculated as scalar values for each design loading case. A NASTRAN scalar point is designated for each design constraint and used as a placeholder for these responses. Displacement design constraints are defined on the displacements of these scalar points.

IV. Program Flow

The new antenna analysis and sensitivity code have been implemented into MSC/NASTRAN, Version 67.5. The new code has been installed and tested on the JPL Cray Y-MP supercomputer and a Silicon Graphics (SGI) Crimson model workstation.

The general flow of the NASTRAN design optimization solution sequence (for statics) is

(1) Read and collate input data.

(2) Update geometric and structural matrices and tables.

(3) Solve for static responses.

(4) Determine sensitivity of objective and constraint functions to design variables.

(5) Perform optimization.

The objective is usually to minimize structure weight, with constraints on antenna performance and element stresses. Steps (2) through (5) are iterated until the design problem converges.

The new antenna analysis and design code are inserted into the NASTRAN design optimization solution sequence in two places: at the end of statics analysis, step (3) above, and after the sensitivity analysis calculations, step (4) above.

At the end of step (3), the new code performs some input data checking, initializes and saves invariant antenna analysis data, and echoes various antenna description and processing parameters to the print file. At this point, all statics response quantities are available and static antenna analyses are performed. The resulting scalar quantities are inserted into the appropriate displacement vectors for each loading case.

Design sensitivity analysis [6], step (4) above, computes the rate of change in structural response to changes in design variables. Small perturbations to the design variables are approximated in the structural matrices, and response derivatives are explicitly solved for. The result, for the statics case, is a set of displacement derivative vectors for each design variable for each loading case. Path-length and pointing-error analyses are performed on each of these displacement vectors, as appropriate. The original statics errors are subtracted to give the change in antenna performance for variations in the design variable. These resulting scalar quantities are inserted into the displacement vectors for each loading case and passed to the optimizer.

The added antenna analysis and design codes do not modify or interfere with the operation of the original optimization code and are compatible with all the other sensitivity and design options in the design optimization solution sequence. The advent of geometry optimization in the next release of MSC/NASTRAN is especially intriguing. The method employed is extensible to constraints on other performance and operational measures, e.g., secondary reflector offsets or geometric theory of diffraction (GTD) performance analyses.

V. Effectiveness

JPL-ANTOPT is intended eventually to supplant the JPL-IDEAS program. Test design optimization runs have been made using a small verification model (Fig. 1) and the IDEAS design model for the new DSS-24 34-m antenna (Fig. 2). These models are summarized in Table 1. (The numbers in square brackets are the number of design variable linking groups in each element type. Path-length error constraints (P/L) are in mm rms. Pointing errors (PNT) are in arc-sec.)
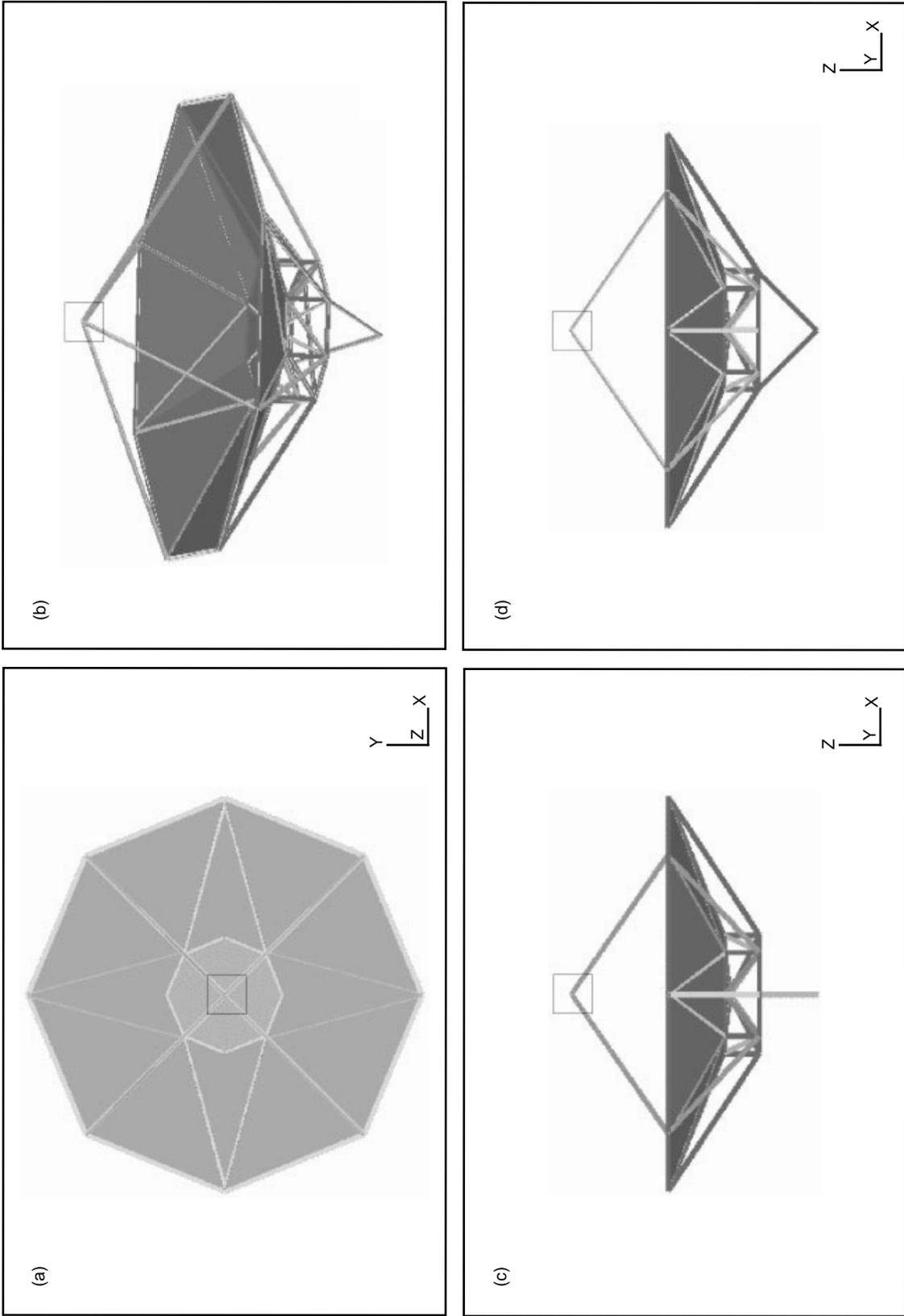
Fig. 1. Test model: (a) plan view, (b) partial rotation, (c) back elevation, and (d) side elevation.
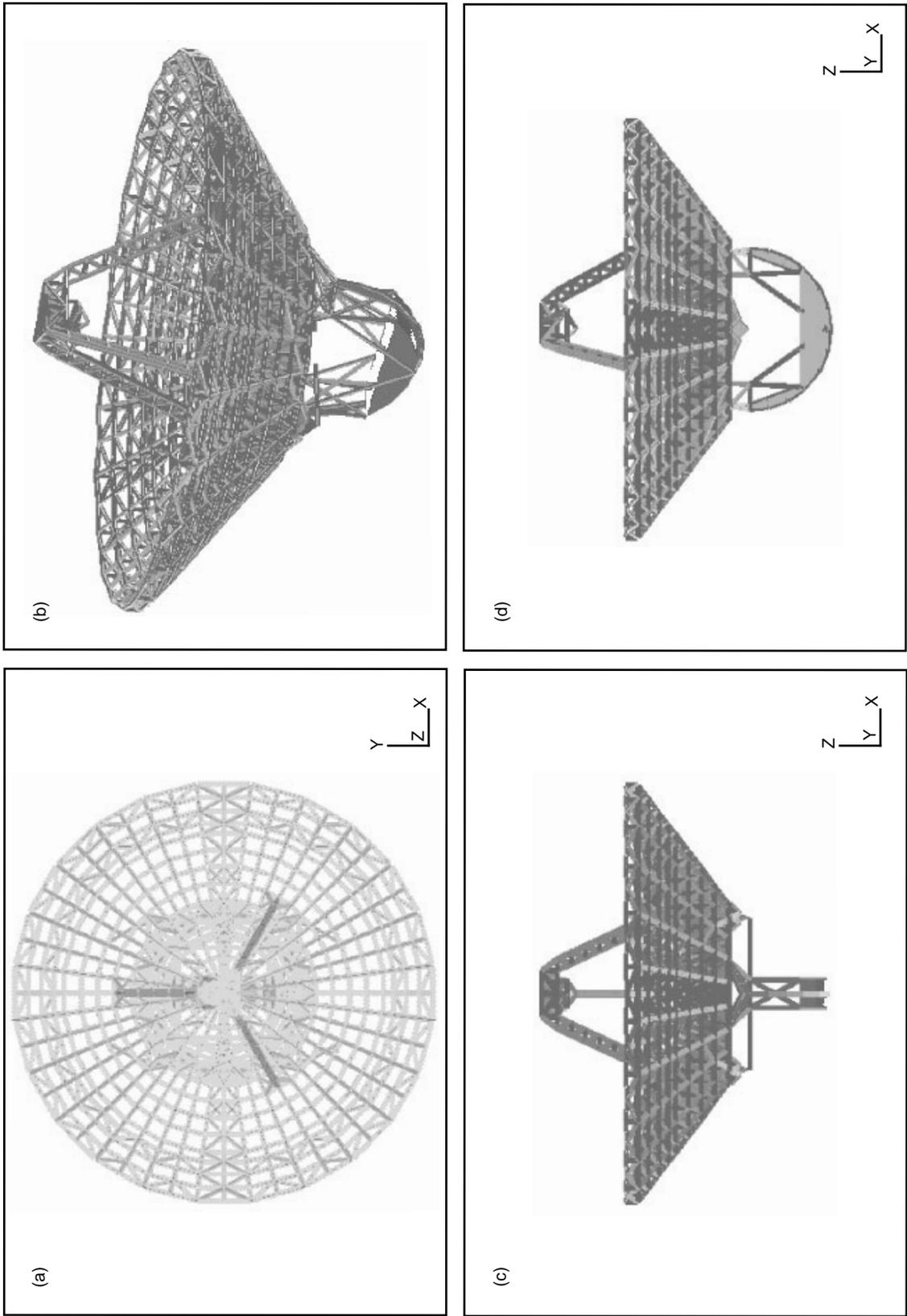
(a)

(b)

(c)

(d)

287

Fig. 2. The 34-m model: (a) plan view, (b) partial rotation, (c) back elevation, and (d) side elevation.

Table 1. Comparison model summary.

Component	Test model	34-m model
Grids	28	1473
Elements		
Rod	88 [12]	3876 [243]
Tri		106 [10]
Quad		562 [29]
Mass	18	1127
Design constraints		
Z-gravity P/L	0.254	0.381
Y-gravity P/L	0.254	0.381
Y-gravity PNT	50.0	900.0
Rim $+Z$ force PNT	50.0	
S/R $+Y$ force PNT	100.0	

Design constraint values were chosen to exercise the programs and have no other significance. For the baseline configurations, each constraint is violated by a factor of from 1.5 to 4. Stress and other side constraints were disabled. The default optimizer input parameters were used for both programs except that termination of design iterations due to meeting convergence criteria was prevented.

The design variables for each model are the cross-sectional areas of the rods and thicknesses of the plates. Minimum and maximum design variable limits were imposed: for the test model rod areas, 64.5 mm^2 and 6451.6 mm^2, and for the 34-m model, 322.6 mm^2 and 32258.0 mm^2 for the rod areas and 2.54 mm and 254.0 mm for the plate thicknesses. Some of the structure model was excluded from the optimization problem, including lumped masses that were used to account for the weight of the main reflector panels, secondary reflector, and counterweight; the remainder is deemed the variable structure.

Three comparative design optimization runs were performed using each model. The baseline configuration for the test model was uniform rod areas of 645.2 mm^2; that of the 34-m model was 3225.8-mm^2 rod areas and 25.4-mm plate thicknesses. In addition, starting points of minimum and maximum design variable sizes were used. The geometry and element connectivity were not changed.

Figures 3 and 4 are plots of the variable and feasible structure weights as functions of design iteration history for the six optimization runs for each program. Feasible structure weight is the variable structure weight scaled by the largest ratio of performance measure to design constraint. For example, if a design constraint were violated by 10 percent at a particular iteration, the feasible weight would be 110 percent of the variable structure weight. The ratio of feasible to variable weights, then, is proportional to the worst constraint violation. The individual curves in the plots are designated I-WGT and I-Feas for variable structure weight and feasible weight as reported by the IDEAS program, and A-WGT and A-Feas for the weights reported by the ANTOPT program. (The differences between the initial feasible weights of the IDEAS and ANTOPT 34-m model runs is attributable to the differences in the weight and stiffness characteristics of the plate elements in the two programs.) It can be seen that the new program consistently achieves a feasible design in a few iterations.

JPL-ANTOPT comprises over 1800 lines of MSC/NASTRAN DMAP source code and has been accepted by NASA's Computer Software Management and Information Center (COSMIC) as program NPO-19349.

VI. Summary and Conclusion

The JPL-ANTOPT program performs microwave antenna performance analysis and structure optimization in an efficient manner that is easy for the structure designer to use. The new code is portable
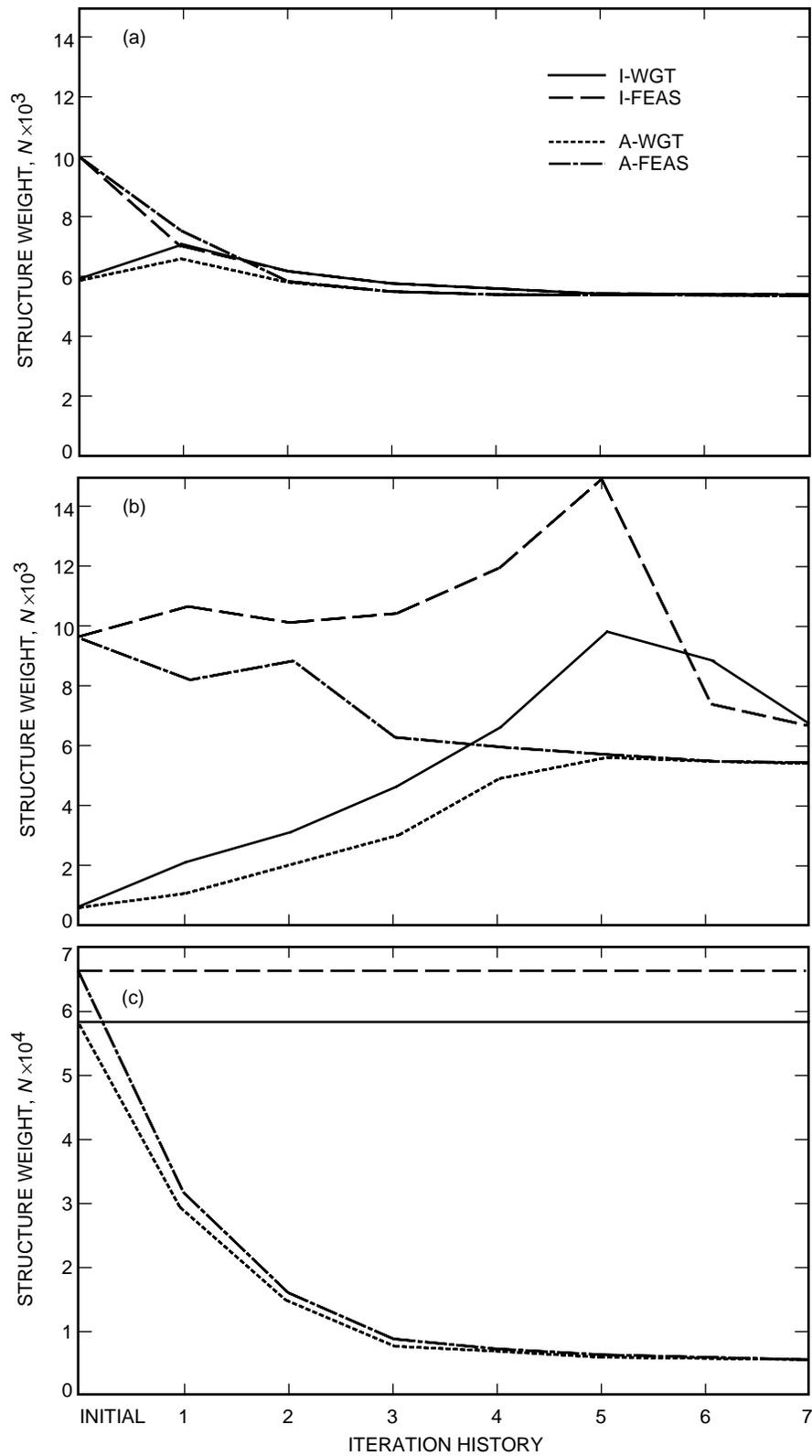
Fig. 3. Test model weight history: (a) initial = baseline; (b) initial = minimum; and (c) initial = maximum.
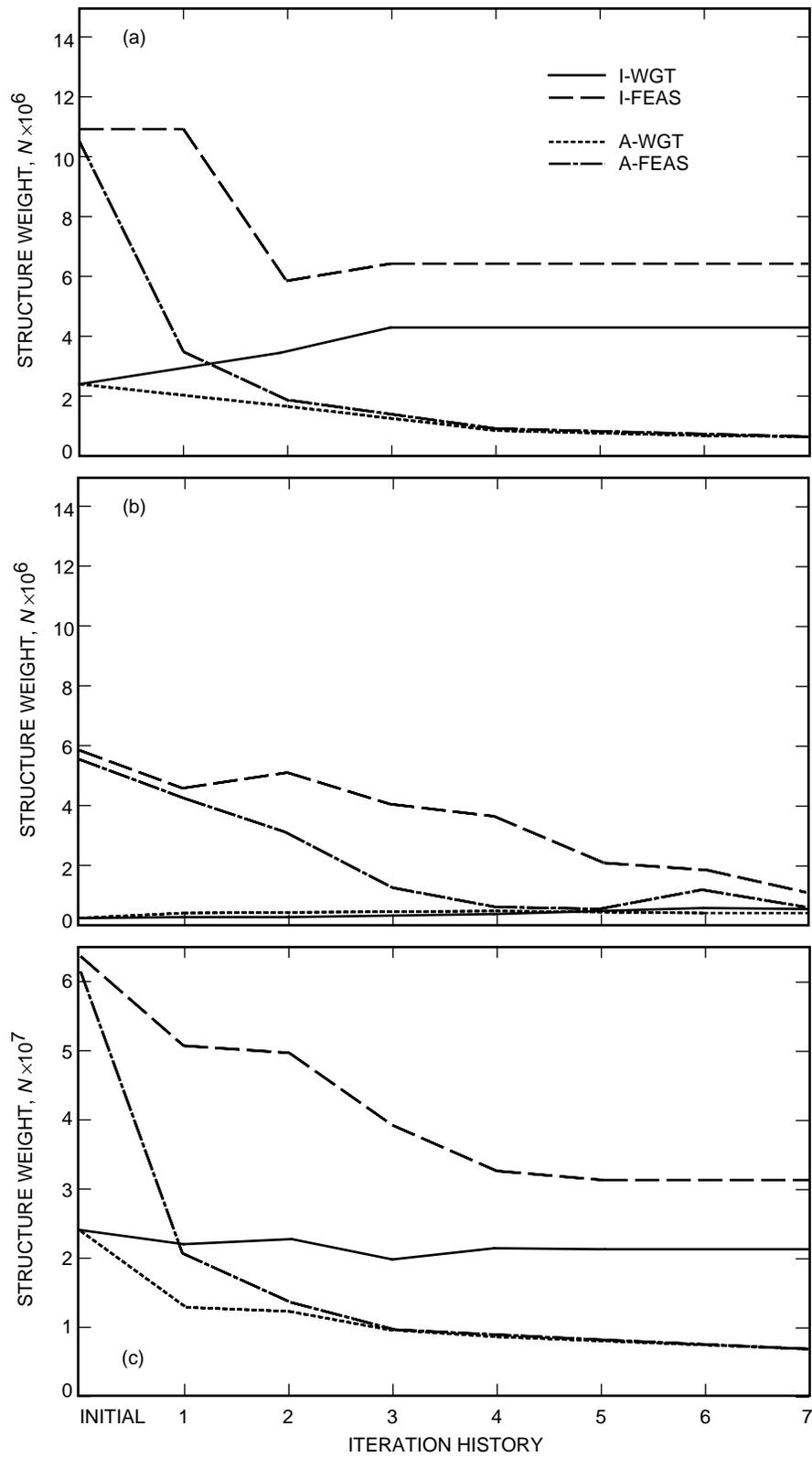
Fig. 4. The 34-m model weight history: (a) initial = baseline; (b) initial = minimum; and (c) initial = maximum.

across computer platforms and is compatible with other NASTRAN optimization capabilities. The method employed to introduce antenna performance measures into the NASTRAN optimization sequence is easily adaptable for use with other performance measures.

References

[1] R. Levy and D. M. Strain, *User's Manual for the JPL-IDEAS Finite Analysis and Design Optimization Program*, COSMIC NPO-17783, NASA Software Technology Transfer Center, University of Georgia, Athens, Georgia, October 1988.

[2] S. M. Barondess and S. Utku, *Computation of Weighted Root Mean Square of Path Length Changes Caused by the Deformations and Imperfections of Rotational Paraboloidal Antennas*, JPL Technical Memorandum 33-118, Jet Propulsion Laboratory, Pasadena, California, March 1, 1963.

[3] M. S. Katow and L. Schmele, "Utku/Schmele Paraboloid RMS Best-Fit Program," *Computer Programs for Antenna Feed System Design and Analysis, Vol. 1: Programs and Sample Cases*, A. Ludwig, ed., JPL Technical Report 32-979, Jet Propulsion Laboratory, Pasadena, California, pp. 75–82, April 15, 1967.

[4] J. Ruze, *Small Displacements in Parabolic Reflectors*, Massachusetts Institute of Technology, Lincoln Laboratory, Lexington, Massachusetts, February 1, 1969.

[5] *MSC/NASTRAN Quick Reference Guide, Version 67*, MacNeal-Schwendler Corporation, Los Angeles, California, 1992.

[6] G. J. Moore, *MSC/NASTRAN Design Sensitivity and Optimization User's Guide, Version 67*, MacNeal-Schwendler Corporation, Los Angeles, 1992.